



Trade Science Inc.

# Materials Science

*An Indian Journal*


---

**Full Paper**

MSAIJ, 4(1), 2008 [33-40]

## Modeling and studying of the fatigue behavior of the composite coated steel

Issam S.Jalham\*, Ahmad O.Hasan

Industrial Engineering Department, Faculty of Engineering and Technology,

University of Jordan, Amman 11942, (JORDAN)

E-mail: jalham@ju.edu.jo

Received: 2<sup>nd</sup> July, 2007 ; Accepted: 7<sup>th</sup> July, 2007

### ABSTRACT

In this study the Plasma spray coating method was used to melt the coating powder material and spray it on to the surface of the steel substrate. The coated specimens of different pure and composite materials were tested under the standard fatigue testing conditions. The best results were observed for the specimens coated with pure molybdenum followed by those coated with copper-bronze, while the worst behavior was that of the specimens coated with 100% ceramic materials. SEM test was conducted to understand the reasons behind this behavior. It was found that this behavior is due to the initiation of the crack along the boundary of the smooth area for the coated specimens, which takes time to propagate, while for the uncoated specimen the crack initiated at the boundary between the smooth regions and propagates radial inside it. The mathematical model of the behavior  $\sigma_a = K(2N_f)^b$  is found to suit the results of the fatigue test for all coated and uncoated specimens regardless if there is an improvement or not in the fatigue behavior.

© 2008 Trade Science Inc. - INDIA

### KEYWORDS

Plasma;  
Coating;  
Composite;  
Scanning electron microscope;  
Modeling;  
Crack.

### INTRODUCTION

It is known that many components are subjected to alternating or fluctuating loading cycles during service, and failure by fatigue is fairly common occurrence because cyclic loading produces microscopic surface discontinuity resulting from dislocation slip steps that ends with a crack initiation<sup>[1]</sup>. It can also be noted that the formation of dislocation slips can be hindered by introducing a two phase structure in the material<sup>[2]</sup>. Coating may provide steel with compressive residual stresses that improves its fatigue life. To increase the fatigue life, different coating materials and techniques can be used.

One of these techniques is plasma spray coating. It relies on a hot, high speed plasma flame (nitrogen, hydrogen, or argon), to melt a powdered material and spray it on to the substrate. A direct current arc is maintained to excite gases into the plasma state. The high heat plasma enables this process to handle a variety of coating materials, most metals, ceramics, carbides and plastics. Jalham et al.<sup>[3]</sup> have used this method to investigate the influence of different types of composite material on abrasive wear resistance of commercial mild steel and came to very interesting results.

The Surface fatigue phenomenon of Mo and Al-bronze coatings was investigated using two-disc ma-

## Full Paper

chine under various loadings<sup>[4]</sup>. It was found that Mo coatings had superior life to surface failure when compared to Al-bronze coatings under pure rolling and rolling/sliding contacts. This is in agreement with what has been reported by Shakelford<sup>[5]</sup>. Recent evolutions in surface engineering have suggested the use of plasma nitriding, PVD coating and their combination in duplex systems<sup>[6]</sup>. It was found that the employment of gas and plasma nitriding improved the thermal fatigue behavior of the surface of treated steel with respect to an untreated one as thermal cracks were found to remain localized in the compound layer or to stop the interface with the diffusion layer. Ramalho et al.<sup>[7]</sup> presented the influence of the fatigue stress range, normal pressure and amplitude of slip on the fracture life for both coated and uncoated EN H320M steel. They found that Zinc films do not influence the fatigue life of the tested Steel. In another investigation, Nascimento et al.<sup>[8]</sup> stated that the internal residual stresses significantly influence the fatigue strength of coated materials. They found that the effect of tungsten carbide thermal spray coating applied by HP/HV process and hard chromium electroplating for the rotating bending tests, was to decrease the fatigue strength for AISI 4340 Steel and the influence is more significant in high cycle fatigue tests than in low cycle fatigue tests. The decreasing of the fatigue strength was higher in chromium electroplated specimens than tungsten carbide coated specimens. Baragetti et al.<sup>[9]</sup> stated that Any coating system, giving improved wear properties, may drastically reduce the fatigue life of a component, due to crack starting in the coating and propagating in to substrate material. Chrome-plate parts showed improved wear behavior but, also, a shorter fatigue life, with respect to those of uncoated parts.

Several ceramic and ceramic-base composite coatings such as zirconium-based alumina, alumina-titanium, magnesia-stabilized zirconium, fly ash, TiN, TiCN, and other materials were studied. For example, Abdel-Samad et al.<sup>[10]</sup> have investigated the influence of the hot isostatic pressing on thermal fatigue resistance of plasma spraying coatings. They showed that the thermal fatigue resistance of the tool steel had an improvement of 33% using Zirconium-based plasma sprayed coatings in addition to the high wear resistance and good heat transfer resistance. The effect of intrinsic proper-

ties of ceramic coatings such as TiN, TiCN and TiAlN films on fatigue behavior of the commonly used rotor steel, Cr-Mo-V steel, in which test samples have been deposited with ceramic coating layers of 2.5-5 $\mu$ m thick by a filtered arc ion plating was studied<sup>[11]</sup>. In this investigation the coating layer micro-hardness, the characteristics and residual stresses of coating films were determined by X-ray diffraction and the high-cycle fatigue tests under rotary bending and axial constant amplitude loading were conducted. It was concluded that the hardness of coating layers increased approximately by 5-10 times more than that of uncoated substrate depending and large compressive residual stresses appeared on the coating layers. They showed that the fatigue strength of coated specimens is superior to those of uncoated substrate, in particular at long fatigue life. They also reported that the fatigue strength of ceramic-coated material is mainly dependent on the retardation of crack initiation of the substrate by hard coating layers compared to the influence of crack growth resistance by ceramic coatings. On the other hand, it was anticipated that ceramic coating layers are fractured at an early stage of the fatigue process because they are too brittle to accommodate the substrate. Gelf et al.<sup>[12]</sup> used CrN monolithic 5 mm thick, deposited on a substrate of H-11 tool steel. They found that a systematic characterization of the coating cannot neglect the evaluation of the residual stress distribution, induced by the coating manufacturing process because it affects the adhesion between coating and substrate. Ahmed et al.<sup>[13]</sup> has investigated the influence of coating thickness, and contact stress fields on the performance and fatigue modes of thermal spray(WC-12% Co) HV of coatings. They reported that a non-dimensional coating thickness parameter, a part from the detection of a new failure mode (termed spalling), indicate that it is possible to achieve a fatigue life in excess of 70 million stress cycles without failure. This improvement in coating performance was attributed to improved fracture toughness of liquid fuel HVOF coatings.

A deterministic model of fatigue may be considered as a mathematical system which allows one to make accurate predictions about the lifetime of a material or structure, given information about the material properties, details of the geometry, and the actions to which it is subjected. A deterministic model is one such

that if the various parameters are specified exactly, then an exact prediction for the lifetime is obtained. In practice there is a large amount of scatter in observed lifetime data for similar materials under similar conditions. This could be because the true parameters are not known exactly, or because there is a natural variability in the physical system. Such scatter will be addressed in the probabilistic adaptations of some of the deterministic models. The different types of model may be roughly divided into two categories; namely those which are empirical-based on observed data, and constructed to fit the data- and those that are more theoretical-based on some physical reasoning, or mechanism which is known to affect the lifetime.

In order to estimate the reliability of real components which undergo varying conditions and stresses at different times in their lifetime, cumulative damage theories were introduced. The idea behind these is that failure is due to a structure accumulating damage at different stress levels until finally fracture occurs. Initially, it was proposed that such accumulation was just a linear combination of damages, but this was subsequently modified to give a non-linear accumulation rule. A continuous version of the accumulation rule, a damage function, was proposed in the 1950s by Kachanov<sup>[14]</sup>. This whole area is called continuum damage mechanics. The use of the damage function allows one to take into account the many and varied mechanisms that affect useful lifetime. As well as the actual crack growth process, one may be interested in the effect that such things as weather play in the accumulation of damage. Under certain conditions it is possible to calculate the stress experienced at any point within a material, using simple engineering theory. Specifically, if the stress is not too great, the material acts under what is called the elastic regime and elastic fatigue fracture occurs. In such a situation, the stress felt at the tip of a crack can be calculated, and the crack opening force deduced. Using these methods it is possible to determine the rate of crack propagation. However, the material will not always follow elastic behavior, and plastic effects must be taken into account. J-integral methods deal with such a situation<sup>[15]</sup>.

There are many ways to incorporate a probabilistic aspect into a so-called deterministic model. One way to do this is to add random noise to the model. Another

way is to associate a random distribution with the model parameters. Yang et al.<sup>[16]</sup> demonstrates this for a hyperbolic crack growth rate function. Markov chains can be used to model fatigue in materials. The assumption that damage is a function of independent parameters, combined with damage accumulated to date is consistent with the Markov property, and hence such methods are employed in a natural fashion. Of specific interest to this research is work on short cracks by Cox and Morris<sup>[17,18]</sup>. The continuous version, the Markov diffusion, has also been examined. The differential equation approach assumes that cracks grow continuously. In reality, crack growth can be a discontinuous process. In order to model this, it may help to consider growth as a combination of a growth event, together with a certain growth magnitude attributable to that event. Such has been modeled in the cumulative jump models K.Sobczyk, J.Trebecki<sup>[19]</sup>.

A graph of stress versus lifetime constitutes one of the first attempts to quantitatively examine fatigue lifetimes<sup>[20]</sup>. This graph, introduced by August Wöhler in 1858, has since become known as the Wöhler or S-N curve. Although the S-N plot provides an estimate of lifetime for a given stress level, it does not take into account any estimate of uncertainty. S-N-P plots are a probabilistic modification which gives an estimate of probability of failure, conditional on number of cycles and stress level. It should be noted that this is very much an empirical method in the sense that the only variables are time and stress. Calibration of such curves is done by experiment, using test specimens. For the analysis, the following equation, which was also used recently by many researchers such as Saeid<sup>[21]</sup>, may be applied:

$$\sigma_a = K(N_f)^b \quad (2)$$

Where: K and b are constants of the material  $\sigma_a$  is the applied stress  $N_f$  is the number of cycles at failure.

Another common method of estimating lifetime consists of fitting the parameters of a Weibull distribution from test data, and this can yield good predictions in practice.

The objective of this work is to utilize the advantages of plasma coating process to form metal coatings with different types of mixtures of metallic and ceramic particles (such as magnesium zirconate, aluminum-

## Full Paper

bronze and molybdenum, and a mixtures of them) to study the possibility of improving the fatigue behavior of steel. Building a mathematical model to predict the fatigue behavior is also of interest. Wöhler or S-N Curve approach using equation 2 was used in this investigation.

### EXPERIMENTAL

To achieve the objectives of this work, five steps were taken: substrate preparation, preparation of the coating material, equipment setup and testing, coating process, and the testing of the coated substrates. The base substrate used in this research is a commercial free machining mild steel material of a composition shown in TABLE 1. Its preparation was started from decreasing the size to the intended one (Figure 1) and removing all surface oxidation by grit blasting. Thirty minutes before coating, the metal blasting machine was used to remove all the contaminations on the surfaces and then specimens were washed with alcohol to get the substrate ready for the coating process. Then the duplex system coating<sup>[22]</sup> was applied: the substrate is first sprayed with a metallic bond layer of stainless steel (about 350 $\mu$ m) of a composition shown in TABLE 2. Magnesium zirconate powder (10 $\mu$ m), aluminum-bronze powder (45 $\mu$ m), molybdenum powder (30 $\mu$ m), and a mixtures of different proportions of them, as shown in TABLE 3, were prepared as materials for plasma coating. The plasma coating apparatus MITCO 7 BM type was used for coating. The coating process was accomplished with the operational parameters shown in TABLE 4.

The fatigue testing apparatus of WP 140 type (figure 2), with test bar dimensions as shown in figure 1, was used for fatigue testing to record sets of stress-number of cycles data to produce what is called S-N curves. The conduction of the test was started by clamping the sample in the spindle of the apparatus and loading it with a concentrated force at the other end to produce an alternating bending stress. The sample was subjected to a pure reversed bending stress in the machine at a zero mean stress. The amplitude of the reversed stress is infinitely adjustable and the machine switched of automatically if the sample ruptures. The number of load cycles is displayed via a digital counter and regis-

**TABLE 1 : Composition of free machining mild steel used in this investigation**

Substance	Si	Mn	Fe	Cr	Mo	Ni	C	S
Wt%	0.37	1.14	96.565	0.14	0.88	0.62	0.0613	0.22406

**TABLE 2 : Composition of the stainless steel metallic bond layer**

Substance	Cr	Al	Mo	Ni	Fe
Wt%	9.0	7.0	5.5	5.0	balance

**TABLE 3 : Powder proportions used in the plasma coating process**

Group number	Magnesium zirconate %	Aluminum-Bronze %	Molybdenum %	Density g/cc
A	90	5	5	4.65
B	90	0	10	4.77
C	90	10	0	4.54
D	85	10	5	4.77
E	85	5	10	4.89
F	0	0	100	9.0
G	0	100	0	6.7
H	100	0	0	4.3

**TABLE 4 : Operational parameters of the plasma coating process**

Spindle speed to rotate the sample during coating (RPM)	Plasma gas flow (g/h)	Current		Voltage DC (V)	Spray distance (mm)	Spray rate (g/h)	
		DC (A)					
		Ar <sub>2</sub>	H <sub>2</sub>				
15	GH	10.08	1.89	500	70	76-127	0.535

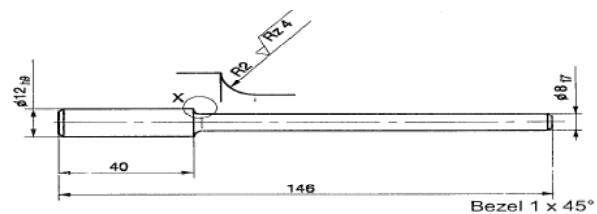


**Figure 1 : Testing bar dimension according to the fatigue testing apparatus of WP 140 type**

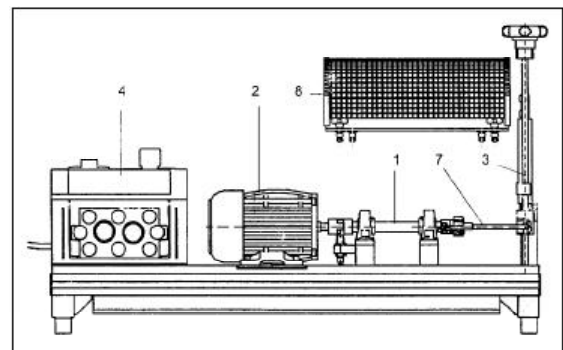


**Figure 2 : The fatigue testing apparatus used in this work. Spindle with sample receptacle (1), Drive motor (2), Load device (3), Switch box with the electrical control and counter (4), extension (7), Protective hood (8)**

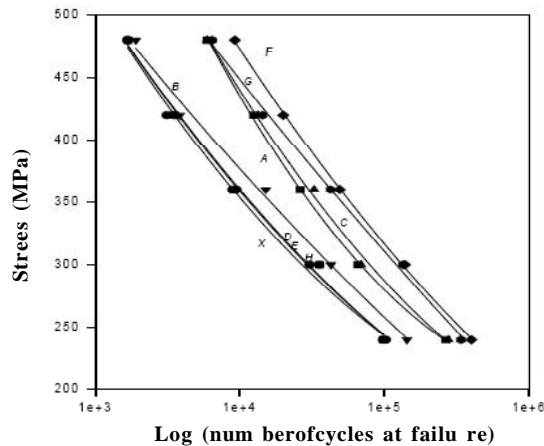


Figure 3 : The relation between the applied stresses and the number of fatigue cycle to failure

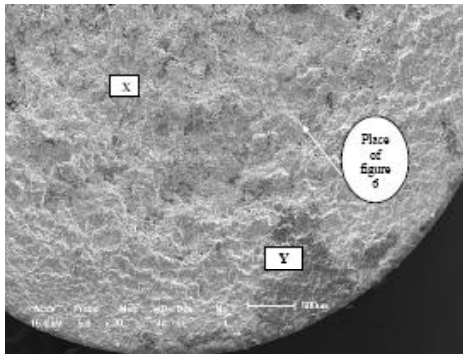


Figure 4 : The two distinguished regions of the uncoated specimen after fatigue testing. X-is the line pattern region, Y- is the granular region, Fatigue stress=200 MPa Magnification 20x

tered for each test.

A selected number of samples were taken to study the mechanism of fatigue using SEM. So, the samples were chosen to cover the substrate before and after coating. For this purpose, the samples that gave the best fatigue behavior and those gave the worst in addition to the uncoated specimens were selected. The samples prepared to conduct SEM test using SHIMADZU SSX-550 Super scan type apparatus.

## RESULTS AND DISCUSSIONS

The relation between the applied stresses and the number of fatigue cycles to failure were plotted for the uncoated and coated specimens tested in this investigation (Figure 3). It is clear that if the test is repeated at higher stress level, the number of the cycles to failure will be smaller. On the other hand, the best fatigue re-

TABLE 5 : Improvement percentages of the fatigue life of the coated materials with relative to the uncoated specimen.

Coating	Improvement %	at Stress (MPa)	480	420	360	300	240
Material							
F	82		84	82	78	74	74
G	74		78	79	77	70	
C	72		77	73	56	63	
A	71		75	66	54	62	
B	12		19	41	29	29	
E	04		12	07	15	03	
D	0.4		11	02	14	-	
H	0.02		09	1.6	12	-	

Note: The order in the table is from the best to the worst.

sults were those of the steel specimens coated with 100% Mo(Group F) followed respectively by those coated of 100% Cu-10 Al powder(Group G), 90% ZrO<sub>2</sub>-24MgO+10% Cu-10Al (Group C), 90% ZrO<sub>2</sub>-24MgO+5% Cu-10Al + 5% Mo (Group A), 90%+10% Mo(Group B), and the slightly better fatigue behavior of those coated with 85% ZrO<sub>2</sub>-24MgO+5% Cu-10Al+10% Mo(Group E), 85% ZrO<sub>2</sub>-24MgO+10% Cu-10Al+5% Mo(Group D), and 100% ZrO<sub>2</sub>-24MgO(Group H). The percentages of improvement at each stress for each material with relative to the uncoated specimen (Group X) are as in TABLE 5. The improvement of the fatigue properties is due to the introduced compressive residual stresses on surface layer. The best results of the specimens coated with pure Mo may be due to its BCC crystal structure because cyclic loading can produce microscopic surface discontinuities resulting from dislocation slip steps which may also act as a stress raiser at the surface, and therefore as a crack initiation sites which is a characteristic of the FCC type of structure due to its high stacking fault energy and rare for this type of structure<sup>[1]</sup>. The copper-bronze mixture coated specimens followed immediately the Mo coated specimens. This is due to the presence of copper which increases the fatigue properties as reported by<sup>[2]</sup>. Moreover, the copper-10Aluminum bronze as an alloy by itself has good fatigue strength as reported in<sup>[4-5]</sup>. The worst behavior under fatigue testing conditions is that of the specimens coated with 100% ceramic materials. These results demonstrate that the ceramic coating layer had more influence on the surface crack initiation during fatigue loading and the ceramic coating layers are fractured at an early stage of the fatigue process because they are too brittle to accommodate the substrate and due to the high difference of ther-

Full Paper

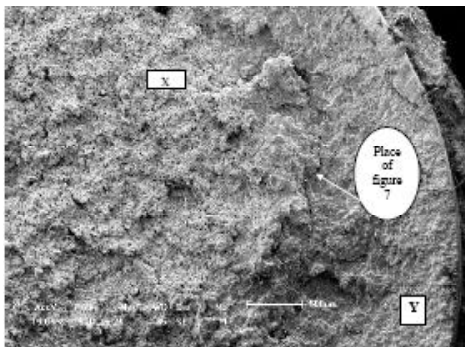


Figure 5 : The two distinguished regions of the coated specimen after fatigue testing. x-is the line pattern region, y- is the granular region, Fatigue stress=240MPa magnification 24x.

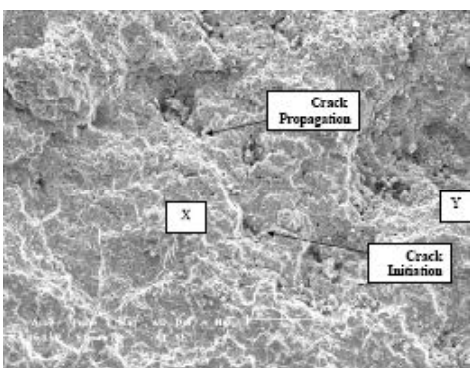


Figure 6 : Cracking in uncoated specimen taken from the site indicated in figure 4, Magnification 50x

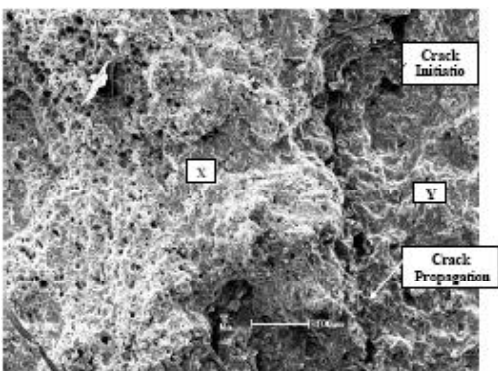


Figure 7 : Cracking in coating specimen taken from the site indicated in figure 5. Magnification 118x

mal expansion that results in the production of unfavorable tensile residual stresses. This is in agreement with Kim et al. [11-12].

The fractured surface of the uncoated specimen, which appeared under the SEM, is shown in figure 4. It is clear that there are two distinguished regions (X & Y). X- region is the smooth region containing curved lines concentric pattern about the crack origin and mark the

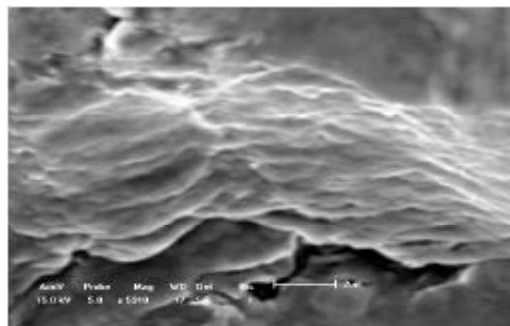


Figure 8 : The slip steps observed the specimens coated with only ceramic material. Magnification 5910x

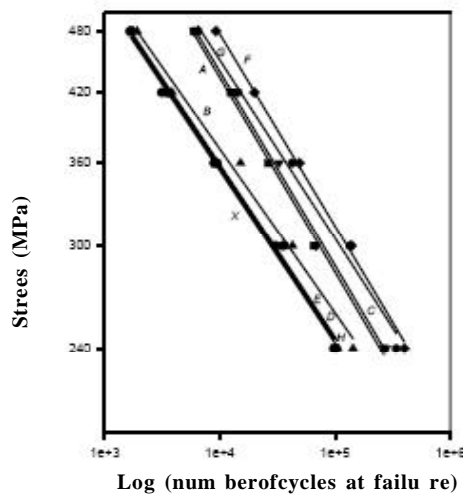


Figure 9 : Log (stress)-log (number of cycles) curves

progress of the crack at various stages. Y- region is the granular region identifies the rapid crack prorogation at the time of failure. The same regions were also clear for the coated specimens that have the best behavior (Figure 5). SEM observations showed that the improvement of fatigue limit of coated samples is due the initiation of the crack along the boundary of the smooth area which takes time to propagate while for the uncoated specimen the crack initiated at the boundary between the smooth regions and propagates radial inside it which speeds up the failure. (Figures 6 and 7), which may explain another reason for the best behavior under fatigue conditions. I.e. the propagation of the cracks took a circular path that gave more life to the specimen before propagating to the surface.

For the specimens coated with only ceramic material, the same regions were observed. It is clear that the slip steps, in the smooth region, are caused by the motion of many dislocations resulting from cyclic loading

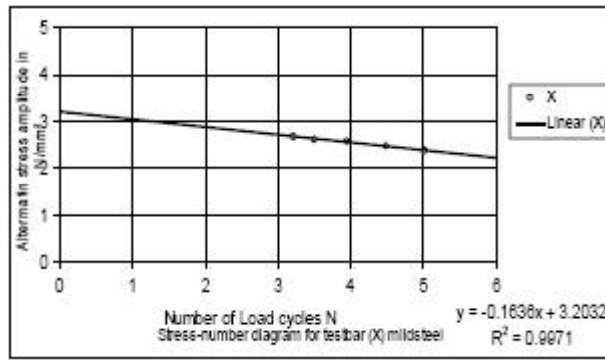


Figure10 : The determination of the constants by using the log-log curves

TABLE 6 : The following table shows the constants K, b,  $\sigma^F$  for the coating groups

Group	Material percentage.	K	b	$\sigma^F$
A	90% (Zro2 24MgO), 05% (Cu 10Al), 05% (Mo)	2332	-0.1819	2701
B	90% (Zro2 24MgO), 0% (Cu 10Al), 10% (Mo)	1613	-0.1605	1736
C	90% (Zro2 24MgO), 10% (Cu 10Al), 0% (Mo)	2296	-0.1805	2728
D	85% (Zro2 24MgO), 10% (Cu 10Al), 05% (Mo)	1701	-0.1704	1815
E	85% (Zro2 24MgO), 05% (Cu 10Al), 10% (Mo)	1702	-0.1692	1813
F	0% (Zro2 24MgO), 0% (Cu 10Al), 100% (Mo)	2573	-0.1839	2900
G	0% (Zro2 24MgO), 100% (0Al), 0% (Mo)	2077	-0.1671	2411
H	100% (Zro2 24MgO), 0% (Cu 10Al) 0% (Mo)	1735	-0.1704	1824
X	(Mild Steel )	1676	-0.1685	1792

TABLE 7 : The fitting equations and the constants as determined by log-log curves

Group	Equation	A	B	R <sup>2</sup>
A	$\text{Log}\sigma_a = -0.1847 \log N_f + 3.3761$	2377.3	-0.1847	0.997
B	$\text{Log}\sigma_a = -0.1556 \log N_f + 3.1918$	1555.2	-0.1556	0.991
C	$\text{Log}\sigma_a = -0.1844 \log N_f + 3.3804$	2401	-0.1844	0.995
D	$\text{Log}\sigma_a = -0.1645 \log N_f + 3.2103$	1622.9	-0.1645	0.994
E	$\text{Log}\sigma_a = -0.1636 \log N_f + 3.2094$	1619.5	-0.1636	0.995
F	$\text{Log}\sigma_a = -0.1823 \log N_f + 3.4076$	2556.2	-0.1823	0.998
G	$\text{Log}\sigma_a = -0.1694 \log N_f + 3.3313$	2144.3	-0.1694	0.990
H	$\text{Log}\sigma_a = -0.1647 \log N_f + 3.2116$	1627.7	-0.1647	0.994
X	$\text{Log}\sigma_a = -0.1636 \log N_f + 3.2032$	1596.6	-0.1636	0.997

(Figure 8). This is common for the ductile engineering materials because the crystal grains that have an unfavorable orientation relative to the applied stress first develop slip steps. Additional slip steps form as more cycles applied and their number may become so large that the rate of formation slows, with the number of slip steps approaching a saturation level. Individual slip bands become more severe and some develop cracks within grains, which then spreads into other grains, joining with other similar cracks, and producing a large crack that propagates to failure. This is in agreement with what has been reported in<sup>[20]</sup>.

For the modeling purposes of the fatigue behavior, the log-log plot (Figure 9) was determined. On this plot, S-N data are found to approximate a straight line. So, Wohler approach using Equation 2 can be applied. Using the log-log plot, the values of A, and the exponent B, were determined according to the approach suggested in<sup>[20]</sup>. In this approach, the slope of the line will give B, and A is the value at  $N_f = 1$  (Figure 10). The results of this approach are shown in TABLE 7.

## CONCLUSIONS

After discussing the results of the achieved work, it can be concluded:

1. The best results were those of the specimens coated with pure Mo followed by those coated with the copper-bronze mixture.
2. The worst behavior under fatigue testing conditions is that of the specimens coated with 100% ceramic materials.
3. The higher the density of the powder, the better the fatigue behavior and the crystal structure of the coating material was found to influence the fatigue properties.
4. SEM observations showed that the improvement of fatigue limit of coated samples is due the initiation of the crack along the boundary of the smooth area which takes time to propagate while for the uncoated specimen the crack initiated at the boundary between the smooth regions and propagates radial inside it which speeds up the failure. The mathematical model of the behavior  $\sigma_a = K(N_f)^b$  is found to suit the results of the fatigue test for all coated and uncoated specimens regardless if there

## Full Paper

is an improvement or not in the fatigue behavior.

5. The constants K and b of the equation in conclusion 4, which are considered as a property of the material, were determined for all coated or uncoated groups.

### REFERENCES

- [1] W.Callister; 'Materials science and engineering', Third edition, John Wiley & sons, Inc, New York, (1994).
- [2] H.Pollack; 'Materials Science and Metallurgy', Third edition, Reston publishing company, Inc. Reston, Virginia, (1981).
- [3] I.S.Jalham, A.Alian; 'Surface wear study of composite spray coated steel', Surface Engineering, **21(5-6)**, 431-438 (2005).
- [4] G.Akdogan; 'Surface fatigue of Molybdenum and Al-bronze Coatings in unlubricated rolling/ Sliding Contact', Wear, **253**, 319-330 (2002).
- [5] J.F.Shakelford; 'Introduction to materials science for engineers', 2<sup>nd</sup> edition, MacMillan, Publishing Company, New York, (1990).
- [6] M.Pellizzari, A.Molinari, G.Straffelini; Surface and Coating Technology, 142-144, 1109-1115 (2001).
- [7] A.Ramalho, L.Corria, J.Costa; Tribology International., **33**, 761-768 (2000).
- [8] M.Nascimento, R.Souza, W.Pigatin, H.Voorwald; International Journal of Fatigue., **23**, 607-618 (2001).
- [9] S.Baragett, G.Vecchia, Terranova; International Journal of Fatigue, **27(10-12)**, 1541-1550 (2005).
- [10] A.Abdel-Samad; Surface and Coating Technology, (2006).
- [11] K.Kim, C.Suh, R.Murakami, C.Chung; Surface and Coating Technology, **171**, 15-23 (2003).
- [12] M.Gelf; Vecchia, N.Lecis, Troglio; Surface and Coatings Technology, **192**, 263-268 (2005).
- [13] R.Ahmad; Wear, **253**, 473-487 (2002).
- [14] L.M.Kachanov; 'Introduction to Continuum Damage Mechanics', Netherlands: Martinus-Nijhoff Publishers, (1986).
- [15] J.R.Rice; Journal of Applied Mechanics, Transactions, ASME, (1968).
- [16] J.N.Yang, G.C.Salivar, C.G.Annis; Engineering Fracture Mechanics, **18(2)**, 257-270 (1983).
- [17] B.N.Cox, W.L.Morris; Fatigue and Fracture of Engineering Materials and Structures, **10(5)**, 419-428 (1987).
- [18] B.N.Cox, W.L.Morris; Fatigue and Fracture of Engineering Materials and Structures, **10(6)**, 429-446 (1987).
- [19] K.Sobczyk, J.Trebecki; Probabilistic Engineering Mechanics, **5(3)**, 102-110 (1990).
- [20] NE.Dowling; 'Mechanical behavior of materials', 2<sup>nd</sup> edition, Prentice Hall Inc., London, (1999).
- [21] T.Saeid, S.Yazdani, N.Parvini-Ahmadi; Surface and Coating Technology, **200**, 5789-5793 (2006).
- [22] J.Kraft, M.Alaya, B.Eigenman, R.Oberacker; Proc.Conf.on 'Ceramic Materials', Berlin, Germany, Berlin University, **11-12**, E34 (2000).
- [23] D.Askeland; 'The Science and Engineering of Materials', 3<sup>rd</sup> edition, PWS Publishing Company, Boston, (1994).